IFP Energies nouvelles International Conference
Rencontres Scientifiques d'IFP Energies nouvelles

This paper is a part of the hereunder thematic dossier published in OGST Journal, Vol. 67, No. 5, pp. 731-875 and available online here

Cet article fait partie du dossier thématique ci-dessous publié dans la revue OGST, Vol. 67, n° 5, pp. 731-875 et téléchargeable ici

Dossier edited by/Sous la direction de : **E. Rosenberg**
IFP Energies nouvelles International Conference/Rencontres Scientifiques d'IFP Energies nouvelles

Pore2Field - Flows and Mechanics in Natural Porous Media from Pore to Field Scale

Pore2Field - Physique des écoulements en milieux poreux naturels : de l'échelle du pore à l'échelle du réservoir

Oil & Gas Science and Technology – Rev. IFP Energies nouvelles, Vol. 67 (2012), No. 5, pp. 731-875

Oil & Gas Science and Technology – Rev. IFP Energies nouvelles, Vol. 67 (2012), No. 5, pp. 737-742

DOI: 10.2516/ogst/2012039

IFP Energies nouvelles International Conference
Rencontres Scientifiques d'IFP Energies nouvelles

Pore2Field – Flows and Mechanics in Natural Porous Media from Pore to Field Scale
Pore2Field – Physique des écoulements en milieux poreux naturels : de l'échelle du pore à l'échelle du réservoir

Molecular Dynamics Simulation of Spontaneous Imbibition in Nanopores and Recovery of Asphaltenic Crude Oils Using Surfactants for EOR Applications

M.R. Stukan[1]*, P. Ligneul[1] and E.S. Boek[2]*

1 Schlumberger Dhahran Carbonate Research Center, Dhahran Techno Valley - KFUPM, P.O. Box 39011, Dammam/Doha Camp 31942 - Saudi Arabia

2 Dept. of Chemical Engineering, Imperial College London, London SW7 2AZ - UK

e-mail: mstukan@slb.com - e.boek@imperial.ac.uk

* Corresponding author

Résumé — Simulations de dynamique moléculaire d'imbibition spontanée dans des nanopores et pour la récupération d'huiles brutes asphalténiques en utilisant des agents tensioactifs pour des applications d'EOR — Nous présentons des simulations de Dynamique Moléculaire (DM) du processus d'imbibition dans des nanopores dans le cas de deux mécanismes différents de modification de mouillabilité. Nous comparons l'imbibition d'une solution aqueuse d'agent tensioactif dans un pore mouillé d'huile entraînée par une adsorption d'agent tensioactif sur la surface de roche mouillée d'huile (mécanisme de revêtement) et l'imbibition d'une solution aqueuse d'agent tensioactif entraînée par des agents tensioactifs éliminant les molécules contaminantes de la surface originellement mouillée d'eau (mécanisme de nettoyage). Nos résultats montrent une différence qualitative en matière de dynamique d'imbibition dans ces deux cas et indiquent que la simulation de DM constitue un outil utile pour étudier les mécanismes d'imbibition à l'échelle des pores avec des implications directes pour des opérations de récupération renforcée d'huile (EOR, *Enhanced Oil Recovery*).

Abstract — Molecular Dynamics Simulation of Spontaneous Imbibition in Nanopores and Recovery of Asphaltenic Crude Oils Using Surfactants for EOR Applications *— We present Molecular Dynamics (MD) simulations of the imbibition process in nanopores in case of two different mechanisms of the wettability modification. We compare the imbibition of an aqueous surfactant solution into an oil-wet pore driven by surfactant adsorption onto the oil-wet rock surface (coating mechanism) and the imbibition of an aqueous surfactants solution driven by surfactants removing the contaminant molecules from the originally water-wet surface (cleaning mechanism). Our results show qualitative difference in the imbibition dynamics in these two cases and indicate that MD simulation is a useful tool to investigate details of the imbibition mechanisms at the pore scale with direct implications for Enhanced Oil Recovery (EOR) operations.*

INTRODUCTION

The re-emergence of interest in EOR has motivated new investigations of the fundamentals of recovery processes in pores of various shapes and wetting patterns [1, 2]. Multi-scale reservoir heterogeneities, typical of carbonates, play a major role in the recovery process. In this frame displacement of oil from oleophilic micropores poses significant challenges due to capillary effects. Many of the chemical EOR methods target interfacial tension reduction or alteration of the wetting state of the matrix from hydrophobic to more hydrophilic by adding surfactants to the injected fluid. Although the chemical agents in solution are injected into the formation by the mean of pressure gradients, diffusion controls the transport of the active chemical agents toward the interface between the injected fluid and the oil entrapped in the pores and pore throats. Since for sub-micron size pore throats the capillary pressure is too high to be balanced by the external pressure gradient, the system evolution is governed by diffusion-limited spontaneous imbibition.

In this study, we consider the processes related to the migration of a fluid in porous media (*e.g.* oil migration in reservoir rocks) at the pore scale. In particular, we investigate the mechanisms of spontaneous imbibition inside pores of nanometer size. In a recent study [3], we investigated in detail how the capillary roughness influences the imbibition rate in capillaries of different wettabilities. We have demonstrated that the capillary rise of a fluid can be perfectly represented by the Lucas-Washburn equation [4, 5] modified [6] to take into account the dynamic contact angle, which is described in the framework of the molecular-kinetics theory [7]. The study demonstrates the relevance of molecular dynamics for the description of the imbibition processes in the case of a simple fluid. The logical next step of the study is to consider imbibition in a multicomponent system such as spontaneous imbibitions in the presence of surfactants and/or asphaltenes.

If the porous medium is exposed to a fluid having an effective contact angle with the matrix smaller than $\pi/2$, the fluid will spontaneously imbibe into the pores. If the effective contact angle is larger than $\pi/2$ the fluid originally contained in the matrix is trapped in the capillaries. To modify the effective contact angle one can use different chemical additives (*e.g.* surfactants). In the current study, we investigate the role of surfactants in the control of the capillary forces (surface alteration) in small oil-wet pore spaces with or without a presence of a crude oil asphaltenic fraction. We considered the following two scenarios:

– imbibition is driven by surfactants adsorption onto the oil-wet rock surface (coating mechanism);
– imbibition is driven by surfactants removing contaminant molecules from the originally water-wet surface (cleaning mechanism).

We have demonstrated a qualitative difference in the imbibitions dynamics in case of coating and cleaning mechanisms of surface alteration. Such a deep understanding of the mechanisms of surface alteration, chemical agents diffusion and spontaneous imbibition dynamics could increase the efficiency of the EOR techniques [8, 9] targeting the rock surface wetting alteration and the reduction of the capillary pressure. This may result in an increase of the production along with an increase of the recovery factor.

1 MODEL

The Molecular Dynamics simulation approach [10] is particularly adapted for investigating the diffusion driven effects at the sub-pore scale (down to nanometers). This modeling technique is extensively used in industry for a detailed description of the processes taking place at the molecular level and when the system dynamics is governed by intermolecular interactions together with thermal diffusion. For the simulation, we used the ESPResSo simulation package [11]. In our study, we used a coarse-grained molecular dynamics approach. In the framework of the coarse-graining approach each particle considered in the simulation represents a group of atoms/molecules of the real chemical compounds. The model used here is based on the coarse-grained model developed by Marrink *et al.* [12, 13] and is an extension of the model we used previously for simulation of spontaneous imbibition in rough capillaries [3]. The simulation particles are mapped to the real atoms/molecules as follows: one aqueous particle in the simulation represents four H_2O molecules. A dodecane hydrocarbon molecule is represented by three "oily" particles which are connected by elastic bonds into a short chain. This means that one hydrocarbon bead in our simulation represents four methylene (CH_2) or/and methyl (CH_3) groups. Our system also contained "heterogeneous" compounds, *i.e.* molecules containing both hydrophilic and hydrophobic groups. Such compounds include:

– surfactants, which are represented by two oleophilic and one hydrophilic beads connected together into a short chain;
– asphaltenes, which are represented as "flowershape" aggregates with oleophilic "leafs" and a highly polar "center".

This architecture of asphaltenes corresponds to the generally accepted island model, see *e.g.* [14]. Please note that the surfactants and asphaltenes considered here are model representation. In future work, we aim to create coarse-grained asphaltene models that are consistent with quantitative molecular representations [14]. The pore throat is also constructed from individual particles. All the coarse-grained particles considered in the simulation are shown in Table 1.

In molecular dynamics simulations, all the thermodynamic properties of the media, such as density, viscosity, surface

TABLE 1

Coarse-grained particles used in the simulation

$4H_2O$ molecules	Pore wall grain	Dodecane molecule	Surfactant molecule	Asphaltene molecule

tension, etc., are maintained by means of both inter- and intra-molecular pair potentials. The system dynamics is then recovered by solving Newton's equations of motion for all the particles in the system. In the current study, all particles are considered to be uncharged (*i.e.* each CG particle represents a group of molecules/atoms with a total charge equal to zero) and the spatial interaction between two CG particles i and j separated by the distance r is represented by a spherically truncated and shifted Lennard-Jones potential:

$$U(r) = \begin{cases} U_{Lj}(r) - U_{Lj}(rc); & r < r_c \\ 0 & ; \; r > r_c \end{cases} \quad (1)$$

where

$$U_{Lj}(r) = 4\varepsilon_{ij}\left[\left(\frac{\sigma_{ij}}{r}\right)^{12} - \left(\frac{\sigma_{ij}}{r}\right)^{6}\right] \quad (2)$$

The parameter σ_{ij}, which defines the effective minimum distance between particles i and j, is the same for all particles (all possible pair interactions) and corresponds to 0.47 nm. This value is also considered as the unit length in the simulation. The cutoff radius was set to $r_c = 2/5532\sigma$ (1.2 nm). The interaction parameter ε_{ij} depends on the types of particles involved in the interaction and characterises the strength of their affinity. The complete set of interaction parameters for all possible pair interactions in the system is a bit different for the cases of coating (no asphaltenes) or cleaning (with asphaltenes) mechanisms of wettability alteration. Both sets are provided in Table 2 (1.0 k_BT corresponds to T = 300 K). Values for Oil-Oil (O-O), Water-Water (W-W) and Water-Oil (W-O) were set according to the original Martini force field [12]. The interaction parameters between the surfactants were adjusted in such a way that no micelles or inverse micelles are formed at the concentration considered here (about 6%). In the molecules consisting of more than one coarse-grained particle (dodecane, surfactants and asphaltenes), the particles are also subjected to 2 types of intra-molecular potentials: bond length potential:

$$U_l(r) = \frac{1}{2}K_l(r-\sigma)^2 \quad (3)$$

and angular potential:

$$U_a(\theta) = \frac{1}{2}K_a(\cos(\theta)-1)^2 \quad (4)$$

TABLE 2

Pair interaction parameter ε_{ij} for spatial interactions (values are in k_BT units). Notation: water (W), oil (O), pore wall particle (PW), surfactant oily tail (SOT), surfactant aqueous head (SAH), asphaltene oleophilic "leafs" (AOL), asphaltene polar center (APC)

	W	O	PW	SOT	SAH	AOL	APC
No asphaltenes							
W	2.00	0.80	1.00	1.60	1.90		
O	0.80	1.36	1.20	1.70	0.90		
PW	1.00	1.20		3.00	1.00		
SOT	1.60	1.70	3.00	1.80	0.90		
SAH	1.90	0.90	1.00	0.90	1.90		
With asphaltenes							
W	2.00	0.80	1.30	1.60	1.90	0.80	2.00
O	0.80	1.36	1.00	1.70	0.90	1.36	0.80
PW	1.30	1.00		1.00	1.30	1.00	3.50
SOT	1.60	1.70	1.00	1.80	0.90	1.70	0.80
SAH	1.90	0.90	1.30	0.90	1.90	0.80	10.0
AOL	0.80	1.36	1.00	1.70	0.80	1.36	0.80
APC	2.00	0.80	3.50	0.80	10.0	0.80	2.00

Here, K_l and K_a are the spring and angular force constants and σ is the angle between two consequent bonds. The spring constant was set to K_l = 1 250 kJ/mol/nm^2 for all bonds. For oil and surfactant molecules, the angular constant was set to K_a = 25 kJ/mol in order to allow a certain flexibility for these molecules. For the asphaltenes, in order to keep the molecules flat and compact, all the neighbour beads of the flower-shape structures were connected by harmonic bonds but the angle potential *(Eq. 4)* is applied only to the angles formed by the following bead triplets: 1-7-4, 2-7-5 and 3-7-6 (see *Tab. 1*). The value of the angular constant in this case is 10 times higher than for the linear molecules, *i.e.* K_a = 250 kJ/mol. The mass of all coarse grained particles in the simulation was considered to be the same. Since one dodecane molecule is represented by three coarse grained oily beads and at the same time one aqueous bead represents four water molecules, the mass of each coarse grained particle is in the range of 60-70 amu (atomic mass units). The equations of motion were integrated with the standard velocity Verlet algorithm [10] with a time step $\Delta t = 0.01t$, where $t = \sigma(m/k_BT)^{1/2}$ is the basic time unit. In our case, t corresponds to 2.25-2.35 ps of real time (depending on whether t is estimated from the MD units or by matching the experimental self- diffusion coefficient, as shown in [3]). In order to link the simulation data to the real physical units, t = 2/3 ps was used. As shown in [3, 12, 13], the physical properties of the base fluid, including density, compressibility, diffusivity and surface tension, are in good agreement with experimental observations under

ambient conditions. Here, in order to speed up the dynamics and to be safe from undesired water freezing and surfactant micellization, the temperature of the fluid was set to 390 K (which corresponds to high downhole temperatures). The temperature was kept constant using the standard Dissipative Particle Dynamics (DPD) thermostat [15, 16] with a friction parameter set to 0.1 and a step-function like weight function with a cut-off equal to r_c. Although at such temperatures, the description of the fluid components using interaction parameters from Table 2 is more qualitative rather than quantitative, it still suits our purpose since at the current stage we would like to analyse the trends. The size of the simulation box was $40\sigma \times 40\sigma \times 210\sigma$. Simulations were performed in the canonical (NVT) ensemble, i.e the number of particles N, volume V and temperature T are kept constant. Periodic boundary conditions were applied in all the directions. To construct the pore throat, we have executed the following protocol. At first, 58 000 Lennard-Jones particles with interaction parameter $\varepsilon = 2.0$ were simulated at temperature $T = 300$ K to form a slab geometry. As a result, an equilibrated liquid slab with bulk number density equal to approximately 0.95 was obtained. The thickness of the slab was about 38σ. After the equilibration, the fluid was frozen and a cylindrical pore of radius $R_{pore} = 10\sigma$ was cut in the slab. To reduce the number of particles in the simulation all the particles for which the distance from the capillary central line was more than 13σ were eliminated. As a result, the width of the capillary wall was 3σ. Such wall thickness guarantees that in case of $r_c = 2.5532$ the fluid particles in the capillary do not feel the presence of the outer wall. To make the system closer to the model of a pore throat, two additional planes of 3σ width perpendicular to the direction of the capillary axis were left around the capillary entry and exit to simulate the surfaces of the pores the pore throat connects. The wall particles were fixed during the run (the limitations and validity of this approach are discussed in details in our recent article [3]). Direct and side views of the pore throat are provided in Figure 1.

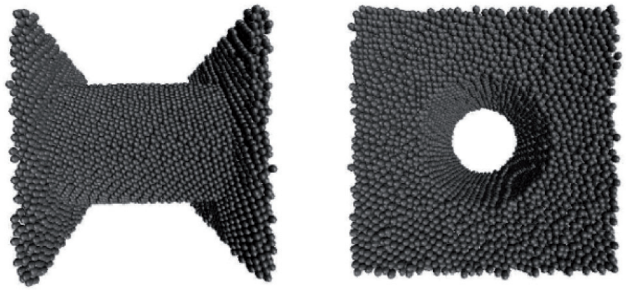

Figure 1

Pore throat and two planes representing the surfaces of the pores connected by the channel.

2 RESULTS AND DISCUSSION

2.1 Spontaneous Imbibition Driven by Surfactant Adsorption

Let us start with the case when the imbibition is driven by the surfactant adsorption on the capillary walls. In this case, the pore throat is originally oil-wet (see *Tab. 2* "No asphaltene" case). At the initial stage the pore throat is filled with oil. The oil also occupies one of the pore volumes (right hand side in *Fig. 2*), while water/surfactant solution fills the other one (left-hand side in *Fig. 2*). In our simulation, the oil phase was represented by 8 000 dodecane molecules (24 000 CG particles). The water/surfactant solution contained 60 000 CG water particles and 1200 surfactant molecules (3 600 CG particles). Thus, the surfactant/water molecule ratio was set to 1:50, which corresponds to about 6wt% concentration for the initial solution.

In the absence of the surfactants in the case of an oil-wet pore throat, the direct extraction of oil by applying an external pressure is almost impossible due to the small pore size and high capillary pressure. However, we can adjust the surfactant properties (by adjustment of the corresponding spatial interaction parameter ε_{ij} (see *Eq. 2*) in such a way that the oleophilic "tails" have a tendency to adsorb at the pore throat surface (see *Tab. 2*). This adsorption will in turn lead to an alteration of the rock surface wettability. The surfactants attach themselves to the surface in a way that their aqueous "heads" are directed towards inner pore volume. This effectively changes the pore throat wettability to more water-wet and thus aids imbibition of the aqueous phase into the pore throat (see *Fig. 2*).

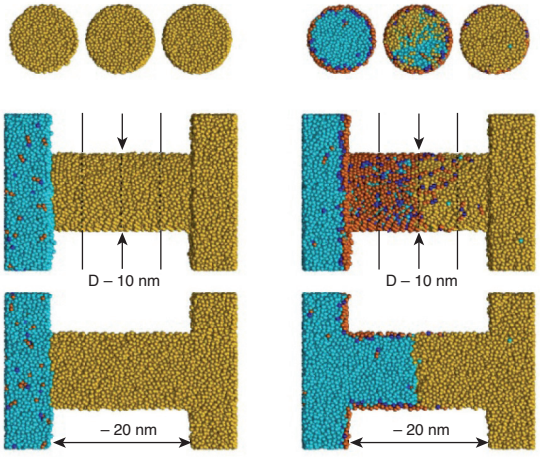

Figure 2

Different stages of imbibition of aqueous surfactant solution in the oil-wet capillary (coating mechanism). Side view (middle), axial section (bottom) and three perpendicular cross sections (top) of the system are shown. All components are shown according to Table 1.

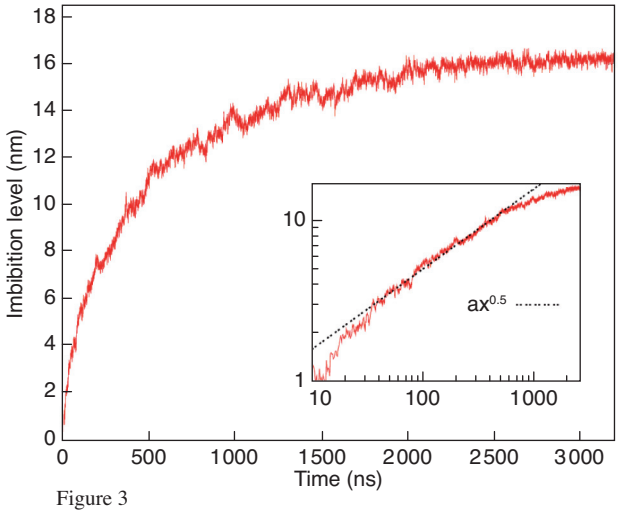

Figure 3

Water meniscus level as a function of time for surfactant imbibition with coating mechanism (capillary is originally oil-wet).

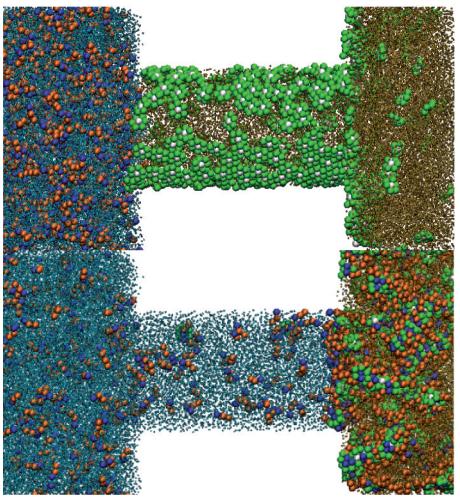

Figure 4

Different stages of imbibition of aqueous surfactant solution (cleaning mechanism) in the capillary rendered oil-wet by asphaltenes (green). Water and oil particles are shown as blue and ochre points respectively; all components are represented according to Table 1.

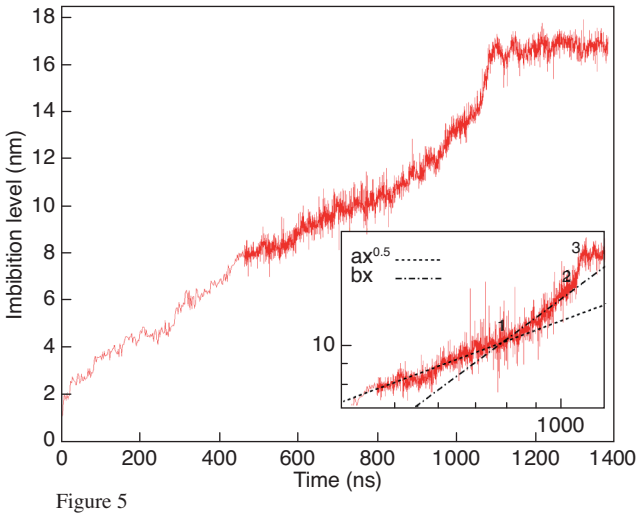

Figure 5

Water meniscus level as a function of time for surfactant imbibition in the presence of asphaltenes (cleaning mechanism).

By monitoring the position of the water-oil boundary in the capillary, we evaluated the imbibition dynamics. It was found that, over a large time span, the imbibition level (meniscus position) is about proportional to the square root of time (see *Fig. 3*) (as in the case of spontaneous imbibition of a single fluid against vapor). These observations are intuitively correct and agree well with known theoretical predictions [17-19]. Deviation from the square-root law at later stages of the rise is related to the decay of the inlet bulk concentration of surfactants, which is considered to be constant in the theoretical studies. The rate of the rise depends in a subtle way on the interaction between the pore wall and surfactant tails. Detailed results on this subject will be presented in the near future [20]. We also would like to note that during the imbibition process the meniscus remains "flat" [21], which is an inevitable consequence of the imbibition mechanism considered here. By adsorption at the triple line surfactants effectively lower the contact angle below 90 degrees so that imbibition occurs. When the meniscus moves the (moving) contact angle increases (dynamic contact angle). However, it cannot increase above 90 degrees since that would lead to retraction of the meniscus. Thus the contact angle remains close to 90 degrees all the time.

2.2 Spontaneous Imbibition Driven by Asphaltene Cleaning

It is assumed that a water-wet rock surface (see *Tab. 2* "with asphaltene" case) was altered (on a geological time scale) from water-wet to oil-wet by adsorption of asphaltenic components on the surface. The pore throat geometry remained the same but during the preparation stage, the pore surface was covered by asphaltenes, which are attached to the water-wet rock by strong interaction between the polar centers of the asphaltenes and the rock surface. The asphaltene/oil molecule ratio was set to 3:80 (300 asphaltene molecules), which corresponds to approximately 15wt%. The number of molecules of all other components remained the same as in the previous subsection. As in the previous case, in the beginning of the simulation the pore throat is filled with oil (see *Fig. 4*). Due to the presence of asphaltenes in the system, it is energetically favourable for the oil to stay in the pore throat. Thus, straightforward forced water imbibition will not be efficient.

Again, surfactants can dramatically change the scenario (as previously, the surfactant/water molecule ratio was 1:50).

In this case, the hydrophilic heads of the surfactants strongly interact with the polar centers of the asphaltenes (see *Fig. 2*). As a result, the surfactants and asphaltenes are arranged in emulsion droplet aggregates, which are soluble in oil. Effectively, the surfactants sweep the asphaltenes off the surface, thus exposing the original water-wet rock to the fluid. This restoration of the original wettability allows water to enter the pore throat and push the oil out. The interaction parameters are set in such a way that without asphaltene in the middle (where it works as an anchor center for hydrophilic sites of surfactants) inverse surfactant micelles are unstable, thus surfactants do not partition into the oil as inverse micelles directly. The detailed analysis of the process of asphaltene desorption is ongoing [20].

The dynamics of the imbibition process is shown in Figure 5. Two different regimes can be seen:

– the imbibition level is proportional to the square root of time (up to point 1 in the graph);
– a pseudo-linear regime occurs from point 1 to point 2.

The final jump (2-3) is related to the surfactant plug escaping from the capillary and is a capillary end effect. The square-root regime agrees well with the theoretical predictions [22], while the pseudo-linear regime requires additional investigation including simulation in longer capillaries to test if it is associated with the finite length of the capillary or not. Nevertheless, one can clearly notice the qualitative difference in the imbibition dynamics between the coating and cleaning cases. In the latter case, the imbibition is much less sensitive to the surfactant concentration, while in case of the coating mechanism, imbibition dramatically slows when the concentration of surfactants decreases. These observations support the recent theoretical predictions [18, 22].

CONCLUSIONS

In the framework of a coarse-grained molecular dynamics approach, we performed a quantitative analysis of the spontaneous imbibition of an aqueous surfactant solution showing two different mechanisms of surface alteration: coating and cleaning. Although the results of the surfactant imbibition should be considered as preliminary, they effectively illustrate the difference between the coating and cleaning mechanisms and show good agreement with theoretical predictions. The results presented here demonstrate the relevance of molecular dynamics simulations for oil recovery research. This is particularly important when one investigates in detail the processes taking place at the nanopores scale where thermal diffusion is the major driving force. Thus, the molecular dynamics approach can be considered as a useful tool to explain the effectiveness of different recovery mechanisms at the molecular scale. The output data of the molecular dynamics simulations can be then used as input parameters in up-scaled models for reservoir simulations.

ACKNOWLEDGMENTS

The authors are grateful to J.P. Crawshaw, P.S. Hammond, A. Clarke and S. Dyer for their comments and stimulating discussions.

REFERENCES

1 Hamida T., Babadagli T. (2007) *Transport Porous Med.* **70**, 231-255.
2 Hamida T., Babadagli T. (2007) *J. Acoust. Soc. Am.* **122**, 1539-1555.
3 Stukan M.R., Ligneul P., Crawshaw J.P., Boek E.S. (2010) *Langmuir* **26**, 13342-13352.
4 Lucas R. (1918) *Kolloid Z.* **23**, 15.
5 Washburn E.W. (1921) *Phys. Rev.* **17**, 273.
6 Martic G., Gentner F., Seveno D., Coulon D., De Coninck J., Blake T.D. (2002) *Langmuir* **18**, 7971-7976.
7 Blake T.D., Haynes J.M. (1969) *J. Colloid Interface Sci.* **30**, 421-423.
8 Puntervold T., Austad T. (2008) *J. Petrol. Sci. Eng.* **63**, 23-33.
9 Strand S., Austad T., Puntervold T., Hognesen E.J., Olsen M., Bastard S.M. (2008) *Energy Fuels* **22**, 3126-3133.
10 Allen M.P., Tildesley D.J. (1987) *Computer Simulation of Liquids*, Clarendon Press, Oxford.
11 Limbach H.-J., Arnold A., Mann B.A., Holm C. (2006) *Comput. Phys. Commun.* **174**, 704-727.
12 Marrink S.J., Risselada H.J., Yefimov S., Tieleman D.P., de Vries A.H. (2007) *J. Phys. Chem. B* **111**, 7812-7824.
13 Marrink S.J., de Vries A.H., Mark A.E. (2004) *J. Phys. Chem. B* **108**, 750-760.
14 Boek E.S., Yakovlev D.S., Headen T.F. (2009) *Energy Fuels* **23**, 1209-1219.
15 Hoogerbrugge P.J., Koelman J.M.V.A. (1992) *Europhys. Lett.* **19**, 155-160.
16 Boek E.S., Coveney P.V., Lekkerkerker H.N.W., van der Schoot P. (1997) *Phys. Rev. E* **55**, 3124-3133.
17 Zhmud B.V., Tiberg F., Hallstensson K. (2000) *J. Colloid Interface Sci.* **228**, 263-269.
18 Hammond P.S., Unsal E. (2009) *Langmuir* **25**, 12591-12603.
19 Hammond P.S., Unsal E. (2010) *Langmuir* **26**, 6206-6221.
20 Stukan M.R., Boek E.S. (In preparation).
21 Blake T.D., De Coninck J. (2004) *Colloids Surf. A Physicochem. Eng. Aspects* **250**, 395-402.
22 Hammond P.S., Unsal E. (2011) *Langmuir* **27**, 4412-4429.

Final manuscript received in April 2012
Published online in November 2012